

SPECTROSCOPIC DISCOVERY OF THE BROAD-LINED TYPE IC SUPERNOVA 2010BH ASSOCIATED WITH THE LOW-REDSHIFT GRB 100316D*

RYAN CHORNOCK¹, EDO BERGER¹, EMILY M. LEVESQUE², ALICIA M. SODERBERG^{1,3}, RYAN J. FOLEY^{1,4}, DEREK B. FOX⁵, ANNA FREBEL^{1,4}, JOSHUA D. SIMON⁶, JOHN J. BOCHANSKI⁷, PETER J. CHALLIS¹, ROBERT P. KIRSHNER¹, PHILIPP PODSIADLOWSKI⁸, KATHERINE ROTH⁹, ROBERT E. RUTLEDGE¹⁰, BRIAN P. SCHMIDT¹¹, SCOTT S. SHEPPARD¹², AND ROBERT A. SIMCOE^{7,13}

Draft version August 15, 2018

ABSTRACT

We present the spectroscopic discovery of a broad-lined Type Ic supernova (SN 2010bh) associated with the nearby long-duration gamma-ray burst (GRB) 100316D. At $z = 0.0593$, this is the third-nearest GRB-SN. Nightly optical spectra obtained with the Magellan telescopes during the first week after explosion reveal the gradual emergence of very broad spectral features superposed on a blue continuum. The supernova features are typical of broad-lined SNe Ic and are generally consistent with previous supernovae associated with low-redshift GRBs. However, the inferred velocities of SN 2010bh at 21 days after explosion are a factor of ~ 2 times larger than those of the prototypical SN 1998bw at similar epochs, with $v \approx 26,000$ km s⁻¹, indicating a larger explosion energy or a different ejecta structure. A near-infrared spectrum taken 13.8 days after explosion shows no strong evidence for He I at 1.083 μ m, implying that the progenitor was largely stripped of its helium envelope. The host galaxy is of low luminosity ($M_R \approx -18.5$ mag) and low metallicity ($Z \lesssim 0.4 Z_\odot$), similar to the hosts of other low-redshift GRB-SNe.

Subject headings: gamma rays: bursts — supernovae: individual (SN 2010bh)

1. INTRODUCTION

While the connection between long-duration gamma-ray bursts (GRBs) and Type Ic supernovae (SNe Ic) has been established in broad terms, the details remain poorly understood (e.g., Woosley & Bloom 2006). Of particular importance is identifying the physical parameter(s) that distinguish the 0.1 – 1% of SNe Ic which give rise to GRBs from those that do not. Related to this question is the diversity within the GRB-SN sample itself. Progress requires detailed spectroscopic observations, which limit in-depth studies of GRB-SNe to the nearest events ($z \lesssim 0.2$). The low detection rate of such events, just ~ 0.3 yr⁻¹, has hampered observational

progress.

Over the past 12 years, detailed spectroscopy has been obtained for just four GRB-SNe: 980425/1998bw (Galama et al. 1998; Patat et al. 2001), 030329/2003dh (Hjorth et al. 2003; Stanek et al. 2003; Matheson et al. 2003), 031203/2003lw (Malesani et al. 2004; Gal-Yam et al. 2004), and 060218/2006aj (Modjaz et al. 2006; Mirabal et al. 2006; Pian et al. 2006). In each case, the spectra revealed unusually broad features, indicative of large ejecta velocities that are faster than 90-95% of all ordinary SNe Ic (Podsiadlowski et al. 2004). Recently, the broad-lined SN 2009bb (Stritzinger et al. 2009) was also shown to produce relativistic ejecta typical of GRBs (Soderberg et al. 2010).

Joining this small set of events, GRB 100316D was detected as an image trigger with the *Swift* Burst Alert Telescope (BAT) on 2010 March 16.531 UT (Stamatikos et al. 2010). The combined pre-trigger BAT survey data and BAT triggered observations revealed a peculiar GRB with a long duration (~ 2300 s), unusual light curve shape, and a soft spectrum (Sakamoto et al. 2010b). A slowly-varying X-ray counterpart was detected with the *Swift* X-ray Telescope (XRT; Starling et al. 2010), but no variable source was detected with the UV/Optical Telescope in early observations (Stamatikos et al. 2010; Oates et al. 2010). These peculiarities resembled the unusual behavior of the low-redshift XRF 060218 (Sakamoto et al. 2010a) and indeed a galaxy at $z = 0.059$ was found inside the XRT error circle (Sakamoto et al. 2010a; Vergani et al. 2010). Follow-up observations with the Gemini-South 8-m telescope revealed a brightening optical counterpart at $\Delta t \approx 1.5 - 2.5$ d after the burst, suggestive of an emerging SN (Levan et al. 2010; Wiersema et al. 2010).

In this Letter, we present our spectroscopic discovery of a SN associated with GRB 100316D

* This Letter includes data gathered with the 6.5-m Magellan Telescopes located at Las Campanas Observatory, Chile.

¹ Harvard-Smithsonian Center for Astrophysics, 60 Garden St., Cambridge, MA 02138, USA, rchornock@cfa.harvard.edu

² Institute for Astronomy, University of Hawaii, 2680 Woodlawn Dr., Honolulu, HI 96822, USA .

³ Hubble Fellow.

⁴ Clay Fellow.

⁵ Department of Astronomy and Astrophysics, 525 Davey Laboratory, Pennsylvania State University, University Park, PA 16802, USA.

⁶ Observatories of the Carnegie Institution of Washington, 813 Santa Barbara Street, Pasadena, CA 91101, USA.

⁷ MIT Kavli Institute for Astrophysics & Space Research, Cambridge, MA 02139, USA.

⁸ Department of Astrophysics, University of Oxford, Oxford OX1 3RH, UK.

⁹ Gemini Observatory, Hilo, HI 96720, USA.

¹⁰ Department of Physics, McGill University, 3600 University Street, Montreal, QC H3A 2T8, Canada.

¹¹ Research School of Astronomy and Astrophysics, The Australian National University, Weston Creek, ACT 2611, Australia.

¹² Department of Terrestrial Magnetism, Carnegie Institution of Washington, 5241 Broad Branch Rd. NW, Washington, DC 20015, USA.

¹³ Alfred P. Sloan Research Fellow.

(Chornock et al. 2010a), subsequently designated SN 2010bh (Bufano et al. 2010; Chornock et al. 2010b), and describe its spectral evolution using extensive optical/near-IR observations spanning 1.47 – 22 days after the burst. As in the case of previous GRB-SNe, our spectra reveal that SN 2010bh is a broad-lined SN Ic. We also find no evidence for helium. The photospheric velocity at late time is significantly higher than even SN 1998bw. Finally, we show that the metallicity of the explosion site is $Z \lesssim 0.4 Z_{\odot}$, in line with the other nearby GRB-SNe host galaxies.

2. OBSERVATIONS

Five observations were performed using the Magellan Echellette (MagE) spectrograph, while single spectra were obtained using the Low Dispersion Survey Spectrograph (LDSS3) and the Inamori Magellan Areal Camera and Spectrograph (IMACS). Two additional epochs of spectroscopy were obtained at later times using the Gemini Multi-Object Spectrograph (GMOS) on Gemini-South. See Table 1 for details.

Standard two-dimensional image reduction and spectral extraction for the long-slit spectra were performed using IRAF¹⁵. Flux calibration and removal of telluric absorption features were performed using our own IDL routines (Matheson et al. 2000). The MagE spectra were reduced using custom IDL scripts. The LDSS3 and IMACS spectra were obtained over a wide wavelength range without the use of order-blocking filters and the effects of second-order light contamination are apparent at long wavelengths; these spectra have been truncated. The optical spectra are presented in Figure 1. All spectra used in this Letter have been corrected for Galactic extinction, which is $E(B - V) = 0.116$ mag for SN 2010bh (Schlegel et al. 1998).

Since we commenced our spectroscopic observations prior to the discovery of a variable source, we oriented the MagE slit for the two initial epochs at a position angle (P.A.) aligned with the majority of the light from the galaxy. This strategy was successful, although it resulted in some contamination from galaxy light across the entire 10'' slit. All subsequent observations were acquired at a more favorable P.A. and clean background subtraction was obtained. The first GMOS spectrum was observed at high airmass with the slit far from the parallactic angle, so its overall spectral slope is less reliable.

We also obtained a single near-infrared (NIR) spectrum on 2010 March 31.15 during commissioning of the new Folded-port InfraRed Echellette (FIRE; Simcoe et al. 2008) spectrograph on the Magellan Baade telescope. We observed the 0.85–2.5 μm range simultaneously, in the low resolution prism mode. The resolution is a strong function of wavelength but is $R = \lambda/\Delta\lambda \approx 2500$ in the J band. Two pairs of exposures with integration times of 600 s and 200 s each were obtained with SN 2010bh nodded along the slit. The OH night sky lines were blended at this resolution and saturated in H and K in the longer pair of exposures, so the effective exposure time at wavelengths longward of 1.4 μm is only 400 s. The signal-to-noise ratio in the SN continuum is therefore quite low

¹⁵ IRAF is distributed by the National Optical Astronomy Observatories, which are operated by the Association of Universities for Research in Astronomy, Inc., under cooperative agreement with the National Science Foundation.

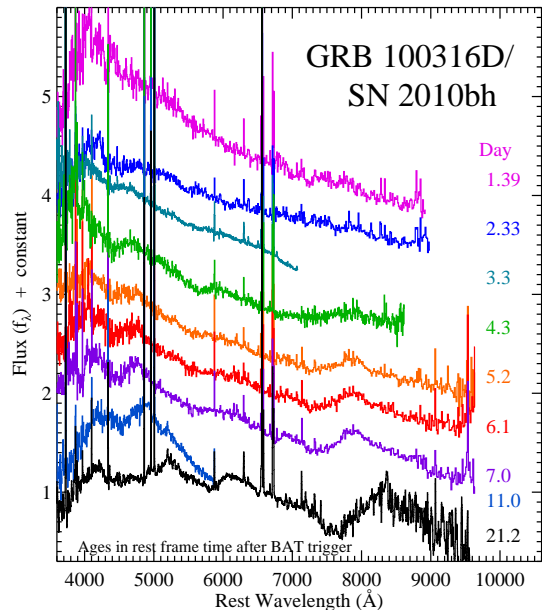


Figure 1. Optical spectra of SN 2010bh from Magellan and Gemini-South demonstrating the emergence of the spectral features of a broad-lined SN Ic. The spectra have been rebinned for clarity. The day 11.0 GMOS spectrum has an unreliable overall spectral shape.

in H and K , but we can clearly detect narrow Paschen- α emission from the host galaxy. We only consider the spectra at shorter wavelengths hereafter. Observations of standard stars were used to apply a flux calibration and correct for telluric absorption.

3. RESULTS

Inspection of the two-dimensional spectroscopic frames reveals that the SN is spatially coincident with bright nebular emission lines of large equivalent width (also visible in Figure 1). Therefore, an H II region and underlying massive star cluster contribute flux to our spectra at an unknown level, particularly the earliest ones when the SN was faint. Observations at late times, after the SN has faded, will be necessary to quantify the contribution of underlying emission to the current dataset, but this does not affect our conclusions below. Fits to the nebular emission lines at the SN location provide a mean redshift of $z = 0.0593$, which we have adopted for the plots in this paper.

3.1. SN Spectral Evolution

The first SN feature present was an absorption dip near 4340 Å on day 2.33 which strengthened and moved redward to 4460 Å by day 7.0. On a similar timescale, a brightening optical counterpart was reported by Wiersema et al. (2010). Combined with the lack of optical variability at earlier times (Oates et al. 2010), we assume negligible contamination from an optical afterglow. Previously, the earliest reported detection of SN features in a GRB-SN was at 1.88 rest-frame days in SN 2006aj (Mirabal et al. 2006), an object which also had a relatively weak optical afterglow from its associated GRB.

The spectral features of broad-lined SNe Ic are highly blended. The most isolated feature is usually taken to be

Table 1
Log of Spectroscopic Observations

| UT Midpoint (YYYY-MM-DD.DD) | Age ^a (days) | Instrument | Exp. Time (s) | Wavelength (Å) | Slit (") | Seeing (") | Airmass | Slit P.A. (°) | Parallactic Angle (°) |
|--------------------------------|----------------------------|------------|------------------|----------------------|-------------|---------------|---------|------------------|--------------------------|
| 2010-03-18.00 | 1.39 | MagE | 1800 | 3300–9500 | 1.0 | 0.7 | 1.1 | 100 | –4 |
| 2010-03-19.00 | 2.33 | MagE | 1800 | 3300–10000 | 1.0 | 0.6 | 1.1 | 100 | –3 |
| 2010-03-20.01 | 3.3 | LDSS3 | 2400 | 3700–7500 | 1.0 | 0.6 | 1.1 | 7 | 5 |
| 2010-03-21.07 | 4.3 | IMACS | 3600 | 3780–9100 | 0.9 | 0.7 | 1.2 | 46 | 41 |
| 2010-03-22.00 | 5.2 | MagE | 1800 | 3300–10350 | 1.0 | 0.9 | 1.1 | 0 | 2 |
| 2010-03-23.00 | 6.1 | MagE | 1800 | 3300–10350 | 1.0 | 0.9 | 1.1 | 0 | 0 |
| 2010-03-24.00 | 7.0 | MagE | 1800 | 3300–10350 | 1.0 | 0.7 | 1.1 | 0 | 3 |
| 2010-03-28.18 | 11.0 | GMOS-S | 1200 | 3400–6230 | 1.0 | 0.7 | 1.7 | 190 | 87 |
| 2010-03-31.15 | 13.8 | FIRE | 1600 | 8500–25000 | 0.6 | 0.6 | 1.6 | 10 | 84 |
| 2010-04-08.00 | 21.2 | GMOS-S | 1200,1200 | 3400–6230,5885–10160 | 1.0 | 0.7 | 1.1 | 190 | 32 |

^a In rest frame, relative to the BAT trigger.

the minimum near 6000 Å, which is commonly identified with Si II λ 6355 (e.g., Patat et al. 2001). That feature is first unambiguously identified in our data on day 4.3 near 5650 Å (blueshift of 35,000 km s^{–1} relative to λ 6355), although the day 2.3 data have a very broad undulation with a shallow dip near 5500 Å (43,000 km s^{–1}). A comparison of this spectrum to other GRB-SNe is shown in the top panel of Figure 2. At similar epochs, SN 2003dh was still completely dominated by the optical afterglow of GRB 030329 (Matheson et al. 2003) while the earliest spectrum of SN 1998bw is from a few days later but shows stronger spectral features. SN 2006aj clearly exhibits lower velocities at this time.

The third emerging SN feature visible in SN 2010bh on day 4.3 is a broad undulation with a minimum near 7070 Å and a flux peak near 7840 Å. Inspection of Figure 1 shows that corresponding features are present in the subsequent MagE spectra and smoothly evolve redward. By day 7.0, the minimum has moved to 7350 Å and the peak is near 7880 Å. A similar feature is present in the SN 1998bw spectrum (Figure 2), and it was identified as a blend of O I λ 7774 and the Ca II NIR triplet at high velocities (Patat et al. 2001).

If we assign the measured absorption minimum in SN 2010bh to O I λ 7774, the implied velocities decrease from 28,300 km s^{–1} on day 4.3 to 16,700 km s^{–1} on day 7.0, values which are low compared to the behavior of the Si II line. One interpretation is that the observed feature is dominated by some other species, such as the Mg II λ 7877, 7896 blend. If the observed feature is in fact primarily due to Mg II, the implied blueshift at absorption minimum decreases from 32,500 km s^{–1} on day 4.3 to 21,000 km s^{–1} on day 7, values which are not only more consistent with those inferred from the Si II line, but also lead to a P-Cygni emission peak near zero velocity.

By the time of our final spectrum, on day 21.2, this feature had morphed into a strong P-Cygni profile with an emission peak near 8300 Å and an absorption component at 7600 Å. These values are too red for O I or Mg II to be contributing significantly to the feature at this time. Instead, it appears to be dominated by the Ca II NIR triplet. Relative to the *gf*-weighted line centroid at 8579 Å, the absorption minimum is blueshifted by 36,000 km s^{–1}. This is a large velocity, but consistent with the value derived from Si II λ 6355 at early times.

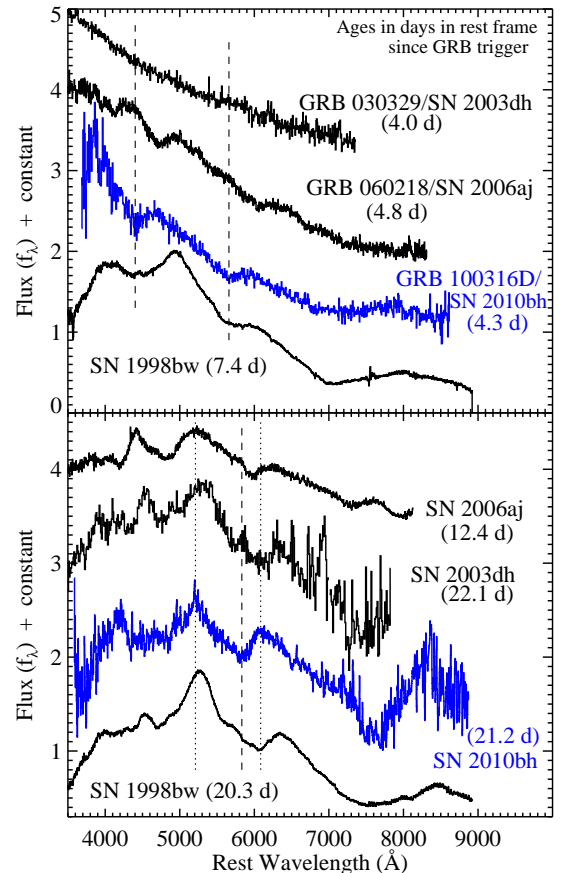


Figure 2. Spectral comparison of SN 2010bh (blue) with other GRB-SNe (Patat et al. 2001; Matheson et al. 2003; Modjaz et al. 2006). Narrow nebular emission lines have been clipped from each spectrum for clarity. *Top:* Early-time spectra. Vertical lines (*dashed*) mark the wavelengths of two absorption features in SN 2010bh. *Bottom:* Spectra taken near 21 days after explosion. The Si II λ 6355 absorption (*dashed*) and two emission peaks (*dotted*) in SN 2010bh are marked. All three features are clearly more blueshifted in SN 2010bh than in the others.

3.2. Large Late-time Velocities

The Si II velocity in SN 2010bh remains large on day 21.2. This can be seen directly in the bottom panel of Figure 2. The vertical dashed line marks the local flux minimum in the SN 2010bh spectrum and it is clearly blueward of the same feature in SN 1998bw at a com-

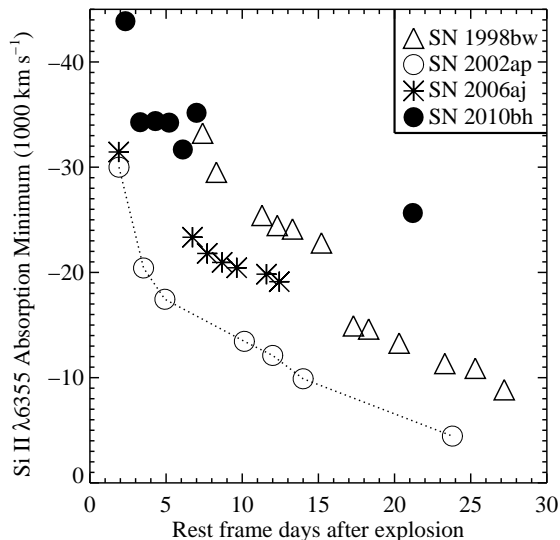


Figure 3. Velocity evolution of the absorption minimum near 5900 Å for several GRB-SNe, assuming that it is Si II $\lambda 6355$ in all objects. SN 2010bh exhibits higher velocities and a shallower decline rate than SN 1998bw at late times, indicative of a higher explosion energy or different ejecta structure. Datapoints for SN 2002ap, which is a broad-lined SN Ic not associated with a GRB, are from the model fits of Mazzali et al. (2002).

parable epoch and SN 2006aj at an even younger age. Quantitatively, the flux minimum is near 26,000 km s⁻¹ (5820 Å), while the minimum in SN 1998bw is blueshifted by only 13,000 km s⁻¹ at this epoch. Similar conclusions can be drawn from the Ca II NIR triplet. As noted above, in SN 2010bh at this epoch the flux minimum is blueshifted by 36,000 km s⁻¹. While the SN 1998bw spectrum is quite blended at these wavelengths and a broad local minimum is present near 7500 Å, another absorption notch is present near 8120 Å, which corresponds to a velocity of 16,400 km s⁻¹ relative to Ca II. This notch clearly develops into the Ca II absorption minimum at later times (Patat et al. 2001).

To make a quantitative comparison, we plotted the velocity evolution of the $\lambda 6355$ feature in Figure 3 compared to SN 1998bw and SN 2006aj; the features in SN 2003dh are difficult to measure against the dilution of the GRB afterglow. Also plotted are velocities for the broad-lined SN Ic 2002ap, which had lower late-time velocities than the GRB-SNe despite the high early-time velocities. While we do not have the same sampling as the SN 1998bw observations, the rate at which the velocity of the Si II feature decreased with time is lower in SN 2010bh, possibly indicating a different ejecta structure or a more powerful explosion, although complications such as potential differences in the ejecta mass preclude any firm statements.

SN 2010bh also differs from SN 2003dh and SN 2006aj (while resembling SN 1998bw) in its lack of an emission bump near 4500 Å (Figure 2). This feature has also been seen in broad-lined SN Ic not associated with GRBs, such as SN 1997ef (Iwamoto et al. 2000) and SN 2002ap (Foley et al. 2003). Even normal-velocity SNe Ic such as SN 1994I (Filippenko et al. 1995) have an emission peak near these wavelengths. Due to the highly blended nature of the spectral features in broad-lined SNe Ic, the emission peaks represent minima in the line opac-

ity rather than emission features from a single transition (e.g., Iwamoto et al. 2000). The lack of the 4500 Å feature in SN 2010bh at an epoch where it is present in other SNe Ic may therefore be another consequence of the unusually high velocities at late times if the iron lines to the blue and red of this wavelength are still blended together. Similarly, the emission peaks present in SN 2010bh near 5200 Å and 6085 Å on day 21.2 are more blueshifted than in the other objects at that time.

Two caveats for this analysis are that the Si II line could be blended with other features in a manner that compromises our velocity measurements or the Si II line-forming layer could be unrepresentative of the true photospheric velocity at late times. However, we believe the combined evidence favors significantly higher velocities in SN 2010bh than SN 1998bw at late times. We note that effects of SN explosion asphericity (Maeda et al. 2006) also could complicate the interpretation of these velocity measurements, but that nebular-phase spectroscopy will offer some insight on the explosion geometry (e.g., Mazzali et al. 2005).

3.3. NIR Spectrum and Lack of Evidence for He

Our goal in obtaining the FIRE spectrum was to test for the existence of helium in SN 2010bh. The presence or absence of helium is a significant constraint on the nature and evolutionary state of GRB progenitors prior to the explosion. Absence of helium is difficult to deduce from optical spectra alone, both due to the high degree of line blending and the general need for non-thermal excitation of the optical lines (e.g., Lucy 1991). Both of these concerns are mitigated by searching for the lower-excitation He I lines at 1.083 and 2.056 μ m in the less-blended NIR part of the spectrum. Furthermore, detection of these NIR lines is substantially more difficult for GRB-SNe at high redshift, so nearby objects represent our best chance to constrain the presence of helium in GRB progenitors. Patat et al. (2001) claimed that both of these lines were present in SN 1998bw, although the weakness of the observed 2.056 μ m line has made this result controversial.

Our FIRE spectrum is shown in Figure 4 and includes the wavelength region around the 1.083 μ m line of He I. A broad spectral feature is present with a peak near 1.02 μ m and an absorption minimum to the blue near 0.95 μ m. We have also plotted the earliest SN 1998bw NIR spectrum, with the absorption minimum at 1.02 μ m identified as He I by Patat et al. (2001) labeled. No corresponding feature is present in SN 2010bh. If the feature at 0.95 μ m were identified with He I absorption, the inferred velocity would be nearly 40,000 km s⁻¹, much higher than the photospheric velocity measured in the optical at that time. We conclude that there is no strong evidence for helium in the outer ejecta of SN 2010bh on day 13.8, unless it is present at extremely high velocities.

The identity of the absorption near 0.95 μ m is unknown. SNe Ib/c frequently have an absorption present redward of 1 μ m and several candidate ions have been suggested to contribute to that feature, such as Si I and C I (Gerardy et al. 2004; Taubenberger et al. 2006), although C I would be expected to exhibit other, weaker transitions as well (e.g., Sauer et al. 2006). If the absorption velocity of the feature is similar to that measured for Si II in the optical, the implied rest wavelength is

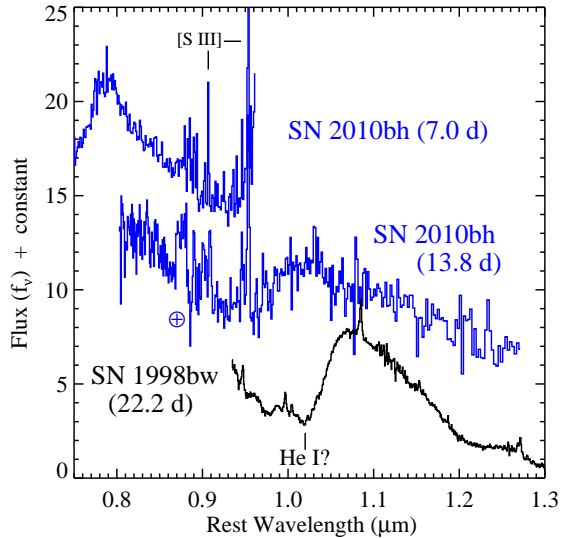


Figure 4. FIRE spectrum of SN 2010bh (middle) compared to the long-wavelength end of the day 7.0 MagE spectrum (top) and the earliest NIR spectrum of SN 1998bw (bottom; Patat et al. 2001). The SN 1998bw spectrum has an absorption minimum near $1.02 \mu\text{m}$ which has been identified with He I $1.0830 \mu\text{m}$, but no clear corresponding feature is present in SN 2010bh. A poorly-removed telluric feature in the SN 2010bh spectra is marked with a \oplus symbol. Two narrow [S III] emission lines from the host galaxy of SN 2010bh are marked.

$1.04\text{--}1.05 \mu\text{m}$.

3.4. Host Galaxy Metallicity

We used the LDSS3 spectrum from day 3.3 to extract information on the bright star-forming region underlying SN 2010bh. The observed ratio of $F_{\text{H}\alpha}/F_{\text{H}\beta} \approx 2.82$ is close to the Case B recombination value, from which we infer that the reddening of the H II region is negligible. The blue spectral shape of the early spectra is an additional argument that SN 2010bh itself suffers low extinction. We estimate an age for the young stellar population of about 6 Myr from the $\text{H}\beta$ equivalent width ($EW \approx 22.8 \text{ \AA}$; Levesque et al. 2010), although this is an upper limit since the SN continuum dilutes the measured EW relative to its true value.

We detect the auroral [O III] $\lambda 4363$ emission line in our spectra. This is often a good indicator of low metallicity because the weakness of the line renders it unobservable in higher-metallicity environments and, indeed, we directly measure $\log(\text{O}/\text{H}) + 12 \approx 7.8$ from the derived electron temperature, T_e . For comparison with studies of previous GRB-SN and long GRB host galaxies (e.g., Levesque et al. 2010), we also derived the metallicity from strong-line diagnostics. Our T_e results place the SN 2010bh environment on the lower branch of the R_{23} metallicity diagnostic (Kewley & Dopita 2002; Kobulnicky & Kewley 2004), which yields a metallicity of $\log(\text{O}/\text{H}) + 12 \approx 8.3$. In addition, we also calculate a metallicity of $\log(\text{O}/\text{H}) + 12 \approx 8.2$ based on the O3N2 diagnostic (Pettini & Pagel 2004)¹⁶. The strong-line diagnostics give $Z \lesssim 0.4 Z_{\odot}$, which is similar to

¹⁶ The T_e -based methods are known to yield systematically lower metallicities than those determined from strong-line diagnostics (Kennicutt et al. 2003; Kewley & Ellison 2008). The metallicities determined here are all consistent with these offsets.

the low-metallicity environments of previous GRB-SNe when placed on the same abundance scales. Additionally, we estimate a total magnitude for the host galaxy of $M_R \approx -18.5$ mag from our IMACS acquisition images, corresponding to $\sim 0.1 L_*$, with some uncertainty due to correction for the emission from the SN.

4. CONCLUSIONS

The spectra presented in this Letter provide conclusive evidence that the $z = 0.0593$ GRB 100316D was accompanied by the broad-lined SN Ic 2010bh. We highlight the following basic properties:

1. Spectral features from SN 2010bh were detected beginning 2.33 days after the GRB, one of the earliest such detections in a GRB-SN.
2. The Si II velocities on day 21 were twice as large as SN 1998bw.
3. The velocity evolution was slower in SN 2010bh than in other GRB-SNe, possibly indicating diversity in the ejecta structure of these events.
4. We find no evidence for helium, indicating a highly-stripped progenitor star.
5. The SN is superposed on a star-forming region with a low-metallicity ($Z \lesssim 0.4 Z_{\odot}$) in a low-luminosity host galaxy.

Continued observations to the nebular phase will shed further light on the ejecta velocity and geometry.

We thank Las Campanas Observatory and the CfA and Carnegie Time Allocation Committees for supporting the Target of Opportunity interrupt observations which made this study possible. We acknowledge the staffs at Magellan and Gemini-South for their assistance with these observations. The MagE reduction routines were modifications of the `mage_reduce.pro` IDL scripts written by G. D. Becker. We acknowledge support from NASA/Swift Guest Investigator grant NNX09AO98G. Some observations were obtained at the Gemini Observatory (Program ID: GS-2010A-Q-5), which is operated by the Association of Universities for Research in Astronomy, Inc., under a cooperative agreement with the NSF on behalf of the Gemini partnership: the National Science Foundation (United States), the Science and Technology Facilities Council (United Kingdom), the National Research Council (Canada), CONICYT (Chile), the Australian Research Council (Australia), Ministério da Ciência e Tecnologia (Brazil) and Ministerio de Ciencia, Tecnología e Innovación Productiva (Argentina).

Facilities: Magellan:Baade (IMACS, FIRE), Magellan:Clay (MagE, LDSS3), Gemini:South (GMOS-S)

REFERENCES

- Bufano, F., et al. 2010, Central Bureau Electronic Telegrams, 2227, 1
 Chornock, R., Soderberg, A. M., Foley, R. J., Berger, E., Frebel, A., Challis, P., Simon, J. D., & Sheppard, S. 2010a, GRB Coordinates Network, 10541, 1

- Chornock, R., Soderberg, A. M., Foley, R. J., Berger, E., Frebel, A., Challis, P., Simon, J. D., & Sheppard, S. 2010b, Central Bureau Electronic Telegrams, 2228, 1
- Della Valle, M., et al. 2003, *A&A*, 406, L33
- Filippenko, A. V., et al. 1995, *ApJ*, 450, L11
- Foley, R. J., et al. 2003, *PASP*, 115, 1220
- Gal-Yam, A., et al. 2004, *ApJ*, 609, L59
- Galama, T. J., et al. 1998, *Nature*, 395, 670
- Gerardy, C. L., Fesen, R. A., Marion, G. H., Höflich, P., Wheeler, J. C., Nomoto, K., & Motohara, K. 2004, in *Cosmic Explosions in Three Dimensions*, ed. P. Höflich, P. Kumar, & J. C. Wheeler (Cambridge: Cambridge Univ. Press), 57
- Hjorth, J., et al. 2003, *Nature*, 423, 847
- Iwamoto, K., et al. 2000, *ApJ*, 534, 660
- Kennicutt, R. C., Jr., Bresolin, F., & Garnett, D. R. 2003, *ApJ*, 591, 801
- Kewley, L. J., & Dopita, M. A. 2002, *ApJS*, 142, 35
- Kewley, L. J., & Ellison, S. L. 2008, *ApJ*, 681, 1183
- Kobulnicky, H. A., & Kewley, L. J. 2004, *ApJ*, 617, 240
- Levan, A. J., Tanvir, N. R., D'Avanzo, P., Vergani, S. D., & Malesani, D. 2010, GRB Coordinates Network, 10523
- Levesque, E. M., Berger, E., Kewley, L. J., & Bagley, M. M. 2010, *AJ*, 139, 694
- Lucy, L. B. 1991, *ApJ*, 383, 308
- Maeda, K., Mazzali, P. A., & Nomoto, K. 2006, *ApJ*, 645, 1331
- Malesani, D., et al. 2004, *ApJ*, 609, L5
- Matheson, T., et al. 2000, *AJ*, 120, 1487
- Matheson, T., et al. 2003, *ApJ*, 599, 394
- Mazzali, P. A., et al. 2002, *ApJ*, 572, L61
- Mazzali, P. A., et al. 2005, *Science*, 308, 1284
- Mirabal, N., Halpern, J. P., An, D., Thorstensen, J. R., & Terndrup, D. M. 2006, *ApJ*, 643, L99
- Modjaz, M., et al. 2006, *ApJ*, 645, L21
- Oates, S. R., de Pasquale, M., & Stamatikos, M. 2010, GRB Coordinates Network, 10520, 1
- Patat, F., et al. 2001, *ApJ*, 555, 900
- Pettini, M., & Pagel, B. E. J. 2004, *MNRAS*, 348, L59
- Pian, E., et al. 2006, *Nature*, 442, 1011
- Podsiadlowski, P., Mazzali, P. A., Nomoto, K., Lazzati, D., & Cappellaro, E. 2004, *ApJ*, 607, L17
- Sakamoto, T., et al. 2010a, GRB Coordinates Network, 10511, 1
- Sakamoto, T., Barthelmy, S. D., Baumgartner, W. H., Cummings, J. R., Gehrels, N., Markwardt, C. B., Palmer, D. M., & Stamatikos, M. 2010b, GRB Coordinates Network, 10524, 1
- Sauer, D. N., Mazzali, P. A., Deng, J., Valenti, S., Nomoto, K., & Filippenko, A. V. 2006, *MNRAS*, 369, 1939
- Schlegel, D. J., Finkbeiner, D. P., & Davis, M. 1998, *ApJ*, 500, 525
- Simcoe, R. A., et al. 2008, *Proc. SPIE*, 7014, 27
- Soderberg, A. M., Nakar, E., Berger, E., & Kulkarni, S. R. 2006a, *ApJ*, 638, 930
- Soderberg, A. M., et al. 2010, *Nature*, 463, 513
- Stamatikos, M., et al. 2010, GRB Coordinates Network, 10496, 1
- Stanek, K. Z., et al. 2003, *ApJ*, 591, L17
- Starling, R. L. C., Evans, P. A., & Stamatikos, M. 2010, GRB Coordinates Network, 10519, 1
- Stritzinger, M., Phillips, M. M., Morrell, N., Salgado, F., & Folatelli, G. 2009, Central Bureau Electronic Telegrams, 1751, 1
- Taubenberger, S., et al. 2006, *MNRAS*, 371, 1459
- Vergani, S. D., D'Avanzo, P., Levan, A. J., Covino, S., Malesani, D., Hjorth, J., & Antonelli, L. A. 2010, GRB Coordinates Network, 10512, 1
- Wiersema, K., D'Avanzo, P., Levan, A. J., Tanvir, N. R., Malesani, D., & Covino, S. 2010, GRB Coordinates Network, 10525, 1
- Woosley, S. E., & Bloom, J. S. 2006, *ARA&A*, 44, 507